

Applied Physics A

A XANES study of chromophores in archaeological glass

--Manuscript Draft--

Manuscript Number:	APYA-D-12-00685R1
Full Title:	A XANES study of chromophores in archaeological glass
Article Type:	SI: SR2A
Corresponding Author:	Rossella Arletti Università di Torino Torino, ITALY
Corresponding Author Secondary Information:	
Corresponding Author's Institution:	Università di Torino
Corresponding Author's Secondary Institution:	
First Author:	Rossella Arletti
First Author Secondary Information:	
Order of Authors:	Rossella Arletti Simona Quartieri, Prof. Ian C. Freestone, Prof.
Order of Authors Secondary Information:	
Abstract:	<p>We applied X-ray Absorption Near Edge Spectroscopy (XANES) to obtain information on the origin of glass color of several archaeological samples and on the oxidation conditions employed during their production. We studied a series of selected glass fragments mainly from excavated primary and secondary production centers and dated to the first millennium AD containing iron and manganese in a wide compositional range. In most of the studied samples iron is rather oxidized, while Mn K-edge XANES data show that, in all the studied glass, Mn is mainly present in its reduced form (predominantly 2+), with the possible subordinate presence of Mn³⁺. The most oxidized samples are the HIMT (High Iron Manganese Titanium) glasses, while the less oxidized belong to the primary natron glass series from the early Islamic tank furnaces at Bet Eliezer (Israel), and to the series coming from a Roman glass workshop excavated in Basinghall Street, London. In these glasses, iron is approximately equally distributed over the 2+ and 3+ oxidation states. The XANES analyses of two glass which had been deliberately decolorized using Sb- and Mn-based decolorizers, demonstrate that Sb is more effective than Mn as oxidant.</p>
Response to Reviewers:	<p>Torino 04/10/12</p> <p>Dear Editor please find enclosed the revised version of the manuscript APYA-D-12-00685 "A XANES study of chromophores in archaeological glass." by Rossella Arletti, Simona Quartieri and Ian Freestone, modified after the reviewers' comments. All the points raised by the reviewers are commented in the following.</p> <p>Editor: The manuscript may look just as "another paper reporting the study of ancient glasses from other provenances" once the novelty eventually contained in the submitted manuscript is not dully emphasized. Beyond complementing the reported chemical data, a more detailed physical discussion of XANES results would help support the submission of the manuscript to Applied Physics A, Materials Science & Processing. -A table with the whole chemical analyses of all the samples was provided -some more details have been added to the description of the method adopted for the determination of Fe oxidation state.</p>

Reviewer #1:

Page 2, line 57-58: It would benefit the readers to include a reference of using arsenic to control the color due to Fe oxidation state as I found it is less common than antimony and manganese for the same role.

-As far as we are aware, arsenic was not used regularly as a decolorant in glass until the eighteenth century AD in Bohemia. It was used on a regular basis in the nineteenth century (see Dungworth D, 2011. The Value of Historic Window Glass. The Historic Environment 2, 21-48). This reference has been added to the manuscript.

Page 3, line 26: Please delete a space before the last bracket.

- The text was corrected according to the referee suggestion

Page 3, line 30: Please use a comma between 20 and 21.

- The text was corrected according to the referee suggestion

Page 4, line 13: The authors used the word "essentially similar technology" referring to a technology applied for production of most glass from the Roman world. This word is rather general and don't provide additional information to the readers. It would be better to describe it or give some reference

-The text has been expanded slightly and rearranged to provide more information

Page 4, line 19: For clarity, please replace "This" with "This workshop".

- The text was corrected according to the referee suggestion

Page 4, line 30-34: The authors suggested a possibility of the furnace having failed towards the end of its life based on color of glass remains. This is very interesting point, but it would be supportive to describe the structure of the furnace, assuming that the authors have investigated the furnace, to understand how the oxygen could leak in, or how it prevented oxygen during its working stage.

-The text has been expanded slightly and rearranged to provide more explanation

Page 4, line 37: Please provide concentration of titanium in the third group of samples studied which were classified as HIMT glass, or at least a range of Ti concentration.

-A table with the whole chemical analyses of all the samples has been included in the manuscript

Page 4, line 59: The authors wrote that Fe and Mn K-edge XANES spectra were collected during two different experiments. Did it mean the Fe spectra were collected using Si(311) and Mn ones using Si(111) crystals?

-Most of the samples (both Fe and Mn K-edges) were collected using a Si(311) crystal. Few samples were collected in a following experiment where only Si(111) was available.

Page 5, line 2: The authors used the photon energy of 7111.5 eV as the first inflection point seen in an Fe-foil XANES spectrum for calibrating the monochromator. The actual value should be 7112 eV. Although it will not affect their analysis as the energy shift due to oxidation state was measured relative to this position, but it is more correct to use the real value.

We are aware that 7112 eV is the actual value of the edge, but, having collected the Fe-foil simultaneously with the samples, and resulting all the foil edges at the same energy position (7111.5 eV), we decided to keep this as the reference value. This choice is, on the other hand, largely adopted in literature.

Page 5, line 10: Replace "XAFS" with "XANES".

-The text was corrected according to the referee suggestion

Page 5, line 21: Please give a reference to the program PeakFit4.

-The reference has been added in the text

Page 5, line 26: Is the uncertainty ± 0.02 eV of the centroid obtained from the fit? How about the uncertainty of the monochromator (photon energy) after calibration? Is this

corrected by measuring a foil placed behind each sample as previously referred to the internal calibration?

- The uncertainty of the monochromator was checked by measuring a foil placed behind each sample. The uncertainty in the energy position of the centroid was estimated by comparing several fit tests.

Page 6, line 2-10: The explanation on how " $I(\text{Fe}^{3+})/[I(\text{Fe}^{2+})+I(\text{Fe}^{3+})]$ " determined is clear enough, but not the "Fe³⁺% from XANES" with the corresponding values listed in the last column of the Table 3. Please explain it.

After this comment, the text and the table were changed.

Page 6, line 43: Please delete a space between "is" and a comma.

- The text was corrected according to the referee suggestion

Figure 4: There are 16 samples in the plot, but 15 samples in the Table 1. Is one of them missing?

-The plot was corrected, the number of samples is 15

Table 1: For not to be mistaken between "not determined" and "not detected", please define "n.d."

-A new table (1) with the whole chemical data was added. The explanation of the abbreviation is given in the caption,

Reviewer #2:

The content and layout of the manuscript are in line with previous papers published by the two first Authors in Archaeometry-focused Journals - namely, references [3-6],[15,16],[22]. Beyond a few specific suggestions that follow, a more detailed physical discussion of XANES data is recommended for a publication in Applied Physics A.

-The XANES data analysis applied in this work is conventional and reported in details in other papers cited here; however, some more details have been added to the description of the method adopted for the determination of Fe oxidation state.

1. Only eight glasses are reproduced in Fig. 1, some with greenish and bluish tonalities; has the bulk chemistry of the glasses been studied? Indeed, to complement the data listed in Table 1 additional chemical information is required concerning the occurrence of other chromophores, particularly copper.

-The detailed chemical analyses was added to the paper, unfortunately, not all the chromophores were analyzed in these specific samples. However, the contexts of the samples and the analyses of closely related material from the same contexts indicate that, apart the North Sinai sample 22, which is cobalt blue, copper and cobalt are present in trace amounts only.

2. To quote the coordination VI for Mn in Table 2 is not enough once the geometry of the coordination environment varies for the listed model minerals (as clearly reflected in the pre-edge details of Mn K-edge XANES spectra reproduced in Fig. 3).

-We are aware that the coordination geometry has an effect on the XANES signal and in fact we have selected several reference compounds containing Mn in different octahedral coordination geometry. However, it must be underlined that, in the present study, we are more interested in the cation oxidation state than in its coordination geometry.

3. Suggestion of a few specific corrections:

- Introduction, p.2, lines 7-8: correct the statement, once the nature of coordinating atoms needs to be known a priori for a full exploitation of XAS data on the absorbing coordinated element - "information about a specific absorbing element: oxidation state, site symmetry, number of surrounding atoms"

-The text has been modified receiving the referee comment. However, it should be noted that with XAS technique (in particular with the study of the EXAFS region of the absorption spectrum), it is also possible to investigate the chemical nature of the neighboring atoms.

- Id., lines 29-30: summarize the references - (e.g., 3 - 22)

-Unfortunately, the software we have used to write the manuscript does not allow summarizing the references.

We sincerely thank the two referees and the Editor for their review work and useful suggestions. We hope the manuscript is now suitable for publication on APA.
Best regards
Rossella Arletti

A XANES study of chromophores in archaeological glass

Rossella Arletti¹, Simona Quartieri² and Ian C. Freestone³,

¹ Dipartimento di Scienze della Terra, Università di Torino, via Valperga Caluso 35, 10125 Torino, Italy

² Dipartimento di Fisica e Scienze della Terra, Università di Messina, Viale Ferdinando Stagno d'Alcontres 31, 98166 Messina S'Agata, Italy

³ Institute of Archaeology, 31-34 Gordon Square, London WC1B 3DG, UK

Running title: XANES study of chromophores in ancient glass

Corresponding author:

Rossella Arletti

Dipartimento di Scienze della Terra, Università di Torino

Via Valpega Caluso, 35 10125 Torino

E-mail: rossella.arletti@unito.it

Phone: +39 011 6705122

FAX:+39 011 6705128

1
2
3
4
5
6
7
8
9
10
11
12
13
14
15
16
17
18
19
20
21
22
23
24
25
26
27
28
29
30
31
32
33
34
35
36
37
38
39
40
41
42
43
44
45
46
47
48
49
50
51
52
53
54
55
56
57
58
59
60
61
62
63
64
65

ABSTRACT

1 We applied X-ray Absorption Near Edge Spectroscopy (XANES) to obtain information on the
2 origin of glass color of several archaeological samples and on the oxidation conditions employed
3 during their production. We studied a series of selected glass fragments – mainly from excavated
4 primary and secondary production centers and dated to the first millennium AD – containing iron
5 and manganese in a wide compositional range. In most of the studied samples iron is rather
6 oxidized, while Mn K-edge XANES data show that, in all the studied glass, Mn is mainly present in
7 its reduced form (predominantly 2+), with the possible subordinate presence of Mn³⁺.
8

9 The most oxidized samples are the HIMT (High Iron Manganese Titanium) glasses, while the less
10 oxidized belong to the primary natron glass series from the early Islamic tank furnaces at Bet
11 Eliezer (Israel), and to the series coming from a Roman glass workshop excavated in Basinghall
12 Street, London. In these glasses, iron is approximately equally distributed over the 2+ and 3+
13 oxidation states. The XANES analyses of two glass which had been deliberately decolorized using
14 Sb- and Mn-based decolorizers, demonstrate that Sb is more effective than Mn as oxidant.
15
16
17
18
19
20
21
22
23
24
25

KEY-WORDS:

26 Archaeological glass, XANES, color, chromophores, iron, manganese
27
28
29
30

INTRODUCTION

31 The elemental composition of early glass is frequently determined in archaeometric studies,
32 in order to obtain information on the raw materials and on their provenance. Less frequently, the
33 oxidation conditions of the glass production are investigated. Actually, the evaluation of the
34 oxidation state of coloring elements in ancient glass offers important information not only about the
35 origin of color, but also on the production technology applied in ancient times. Beyond the choice
36 of the raw materials, oxygen fugacity is one of the parameters which had to be carefully controlled
37 by the ancient glass workers, as this variable was extremely important in determining the final glass
38 color. It is well known, in fact, that the color of glass is largely controlled by the oxidation state and
39 the coordination geometry of the metal ions dispersed in the glass matrix, whether their presence is
40 intentional or unintentional.
41
42
43
44
45
46
47
48
49
50

51 Early glass typically contains 0.3% or more iron oxide, which is able to colour the glass
52 quite strongly, even under moderately reducing conditions. Early glassmakers made various
53 attempts to control the colour due to Fe oxidation state by adding oxides of polyvalent metals,
54 including manganese, antimony and, in the early modern period, **arsenic [1]**. Thus, if we want to
55
56
57
58
59
60
61
62
63
64
65

1 understand the practices of the ancient glass workers and the extent of their control on the final
2 glass colours, we need to systematically study the oxidation state of the glass chromophores.

3 X-ray Absorption Spectroscopy (XAS) is a widely applied technique, able to provide
4 information on iron oxidation states and offers the advantage of being non-destructive, element-
5 selective and sensitive to low concentrations of dilute species. In general, it can provide structural
6 information about a specific absorbing element: oxidation state, site symmetry, **number of the**
7 **surrounding atoms**, inter-atomic distances and disorder parameters of the first few coordination
8 shells. In particular, in the X-ray Absorption Near Edge Spectroscopy (XANES) region of the
9 absorption spectrum (conventionally taken to be within about 50 eV from the absorption edge),
10 characteristic spectral features in the vicinity of the absorption edge are observed. These are due to
11 the electronic transitions from core levels to unoccupied (bound or unbound) final states. These
12 spectral features provide information on the site coordination, symmetry and distortion, and on the
13 oxidation state of the central absorbing atom. A further important characteristic of this
14 spectroscopic technique is its applicability to both crystalline and amorphous materials. For all these
15 reasons, XANES has been successfully applied to a number of archaeological studies (see e.g. 2,3
16 for a review).

17 Concerning Fe-bearing glass of geological or archaeological interest, several XANES studies are
18 reported in literature [e.g. 4,5,6,7,8,9,10,11,12,13,14,15,16,17,18,19,20,21,22,23]. XANES
19 spectroscopy has also been successfully applied to the speciation of Mn in minerals and glass [e.g.
20 24,25,26]), in spite of the difficulties connected with the common co-existence of different
21 oxidation states of this element (2+, 3+, 4+) . In particular, XANES studies of Mn in ancient glass
22 were performed to understand whether this element was present as an impurity in the raw materials
23 or intentionally added to the batch as a decoloring agent (e.g. [6,16,23]. It is, in fact, well known
24 that in ancient times Mn was added as pyrolusite to the batch to control the final color of the glass -
25 by means of a redox reaction in which Mn⁴⁺ reduces while Fe²⁺ oxidizes - neutralizing the effect of
26 Fe²⁺ contained in the heavy minerals present as impurities in the sand, and imparting the typical
27 yellow-green color to the artifacts. Since iron is always present in the ancient glass at measurable
28 concentrations, Fe³⁺/ Fe²⁺ ratio is an appropriate index to compare the oxidation conditions of large
29 suites of archaeological samples .

30 The present paper reports the study of the oxidation conditions of a number of glass finds of the
31 natron type. Natron was a source of sodium carbonate which was found primarily in lakes in the
32 Wadi Natrun and the Nile Delta of Egypt. It was used as a key glass constituent throughout the first
33 millennia BC and AD and is particularly characteristic of Roman glass, the great majority of which
34 was made using natron as a flux. The color of all of the samples here studied derives predominantly

1 from the $\text{Fe}^{3+}/\text{Fe}^{2+}$ ion ratio. This ratio can be determined by i) the raw materials; ii) the furnace
2 atmosphere and melting duration; and iii) any addition of antimony or manganese oxides made to
3 deliberately decolorize the glass by means of iron oxidation.
4

5 **THE ARCHAEOLOGICAL GLASS**

6
7 The analysed samples fall into three groups. A first group of raw glass chunks from Bet Eli'ezer,
8 (Israel, 7—8th centuries AD) – labelled “BET EL” in Table 1 – are derived from a group of
9 primary tank furnaces on the coastal plain of Israel [27]. **It is believed that most glass from the**
10 **Roman world was produced in this region, using an essentially similar technology where**
11 **mineral soda and sand were melted together in large tanks with capacities of 8 tonnes or more**
12 **[27].** Five samples were chosen to give the production color range. A second group of samples are
13 from the excavation of a Roman secondary glass workshop, in Basinghall Street, London (2nd- 3rd
14 centuries AD) – labelled “BAS” in Table 1. This **workshop** used both fresh glass from Palestine
15 and recycled cullet as raw material. The analysed samples were selected to represent a series of
16 stages in the life of the workshop, to determine if significant changes in redox conditions in the
17 furnace occurred. They include raw glass, thought to be imported (BAS 4), and a number of moils,
18 which are the glass remains left around the blowpipe end when a vessel was blown. Among these,
19 two colourless samples – which appear to have been deliberately decolorised by the addition of
20 MnO_2 (BAS 47) and Sb_2O_5 (BAS 46) – were included. **The clay superstructure of the**
21 **reverberatory tank furnace appears to have failed towards the end of its life, allowing air into**
22 **the melting chamber and oxidising the surface layers of the tank of glass from blue to green.**
23 This supposedly “oxidised” glass is represented by sample BAS 71.
24

25
26 A third sample group represents the so-called HIMT glass, (4th-5th centuries AD), which is high in
27 iron, manganese and titanium. HIMT has been suggested to originate in Roman Egypt [28]. One of
28 the HIMT glass here studied was found in Carthage [29] and the other two in the North Sinai [30].
29 Sample NS 6830-22 differs from the others in this study in that it has been deeply coloured by the
30 addition of cobalt.
31

32
33 In addition, to test the origin of its colour, **a chunk of purple plant ash glass** from the early
34 Islamic site of Banias, Israel [26] with high levels of deliberately added manganese, was added to
35 the samples set. **Table 2 reports the chemical data relative to major and minor elements of all**
36 **the analysed samples**
37

38 **EXPERIMENTAL METHODS**

39 *X-ray Absorption Spectroscopy*

40
41
42
43
44
45
46
47
48
49
50
51
52
53
54
55
56
57
58
59
60
61
62
63
64
65

1 Fe and Mn *K*-edge XANES spectra were collected in fluorescence mode at the GILDA-CRG
2 beamline (ESRF, Grenoble, France), during two different experiments, using a dynamically and
3 sagittally focussing monochromator [31], with Si(311) and Si(111) crystals, respectively. For all
4 spectra, a reference metallic foil was used to provide an internal and accurate energy calibration of
5 the monochromator. The position of the first inflection point was taken at 7111.5 and 6538.0 eV for
6 Fe and Mn foil, respectively. The vertical dimension of the investigated regions was about 1mm,
7 while the horizontal one ranged between 2 mm and 5 mm. Beyond the glass samples under study,
8 several model compounds containing iron and manganese in different oxidation states and local
9 geometries were also studied by XANES spectroscopy (see Table 3). All reference compounds [23]
10 were finely ground and deposited on Millipore membranes using alcohols, otherwise the sample
11 spectra were collected directly on the glass fragments. All the XANES spectra were collected at
12 room temperature. The pre-edge background was subtracted and then the spectra of samples and
13 reference compounds were normalized on the high-energy side of the curve. The pre-edge region
14 was then extracted and analysed by least-square fitting of pseudo-Voigt functions (sum of
15 Gaussian and Lorentzian functions) to the pre-edge spectral envelope, using the program PeakFit4
16 [32]. For each sample, the pre-edge centroid was calculated from the average position of the
17 pseudo-Voigt functions, weighted by their respective integrated areas. The estimated error on the
18 centroid position is ± 0.02 . The total integrated area is the sum of the individual integrated areas.

19
20
21
22
23
24
25
26
27
28
29
30
31 The Fe and Mn pre-edge deconvolution of reference compounds and of samples in Fig.
32 2 and 3. The numerical results of the detailed study of the Fe and Mn *K*-edge XANES pre-edges are
33 reported in Table 3 for the reference compounds and in Table 4 for the glass samples.
34
35
36
37

38 RESULTS

39
40
41 It is well known that the Fe *K*-edge XANES spectra display a number of features which may
42 be attributed to transitions between bound electronic states and which shift to higher energies with
43 increasing oxidation state. **In particular, the intensity of the pre-edge peak varies considerably**
44 **as a function of the coordination environment and symmetry**, while the pre-edge energy position
45 is strongly influenced, besides the bond distances, by the oxidation state, being the centroid of the
46 pre-edge peak of the Fe³⁺ rich minerals and glass varieties shifted towards higher energy with
47 respect to those containing iron in the reduced form [19,21,33,34,35,36]. Hence, the centroid energy
48 position is largely used in literature for estimating iron oxidation state. **Moreover, as discussed by**
49 **Wilke et al. [19], the evaluation of Fe oxidation state in glass and melts can be improved**
50 **measuring not only the pre-edge centroid position, but also the intensity values at energy**
51 **positions corresponding to the peak positions of Fe³⁺ and Fe²⁺, respectively. Specifically, good**
52
53
54
55
56
57
58
59
60
61
62
63
64
65

1 results were achieved using the ratios of the intensities measured at these energy positions.
2 Following the procedure adopted in [19] – after determining the centroid energy positions –
3 the pre-edge peak intensities were also calculated by integrating the extracted pre-edge
4 spectra in two energy ranges: (i) between 7113.5 and 7114.5 eV for the contribution of Fe³⁺:
5 I(Fe³⁺) and (ii) between 7111.7 and 7112.7 eV for the contribution of Fe²⁺: I(Fe²⁺). The ratio
6 between the intensities relative to Fe³⁺ and the total iron (*i.e.* I(Fe³⁺)/[I(Fe²⁺) + I(Fe³⁺)]) was
7 then calculated. The percentages of Fe³⁺ in the glass samples was then calculated by these
8 intensity ratios, on the basis of a calibration curve obtained by the references compounds, and
9 then reported in the last column of Table 4. Figure 4 reports the plot of I(Fe³⁺)/[I(Fe²⁺) + I(Fe³⁺)]
10 vs. the pre-edge centroid positions, and shows the good correlation between the results of the two
11 XANES-based methods suitable for estimating iron oxidation state.
12

13 Mn *K*-edge XANES spectra of our glass samples are all very similar . The pre-edge fits (Figures
14 3b) and the energy position of the pre-edge centroids (Table 4) are very similar to those of the
15 reference compounds rhodocrosite and MnO (Fig. 3a and Table 3) which contain Mn in the 2+
16 oxidation state. On the contrary, all the XANES features of pyrolusite (Mn⁴⁺O₂) are shifted by a few
17 eV towards higher energy. These data suggest that, in all the studied glasses, Mn is mainly present
18 in its reduced form, in agreement with the results discussed in literature – see [25] for a review –
19 which report that the high oxidation states of Mn are normally not present in glass because they are
20 unstable at the temperatures at which it is produced. The presence of a subordinate amount of Mn³⁺
21 cannot, however, be excluded, as discussed in [23]. These authors studied a series of Late Roman
22 glass fragments belonging to the HIMT group – coming from archaeological sites in Italy – by
23 means of a multi-spectroscopic approach. They showed that, notwithstanding Mn *K*-edge XANES
24 data suggested the predominant presence of Mn²⁺ in all samples, UV-VIS investigations revealed
25 the presence of minor amounts of strongly coloring Mn³⁺ in some purple glass.
26
27
28
29
30
31
32
33
34
35
36
37
38
39
40
41
42
43

44 DISCUSSION

45 The analysis of the Fe *K*-edge XANES pre-edge peaks (Table 4 and Fig. 2b) indicates that
46 in most of the 15 glass samples here studied iron is rather oxidized. In fact, the position of the pre-
47 edge peak centroid is, for many samples, at higher energy with respect to the standard glass ST1,
48 containing about 70% of Fe³⁺.
49

50 The most oxidized samples are the HIMT glasses (Carthage, NS 6830-27) **the plant ash**
51 **glass from Banias**, and BAS 46 and 47, the colourless glasses from the glass workshop in
52 Basinghall Street, London. Iron oxidation in the fourth century HIMT samples is probably
53 obtained by the deliberate addition of MnO₂, since the amounts of this oxide deriving from the
54
55
56
57
58
59
60
61
62
63
64
65

1
2
3
4
5
6
7
8
9
10
11
12
13
14
15
16
17
18
19
20
21
22
23
24
25
26
27
28
29
30
31
32
33
34
35
36
37
38
39
40
41
42
43
44
45
46
47
48
49
50
51
52
53
54
55
56
57
58
59
60
61
62
63
64
65

chemical analysis are not consistent with its presence as impurity in the raw materials. The strong color of these samples is due to the combination effect of the presence of overall high Fe and Mn contents.

It is interesting to note that the two glass from North Sinai (NS 6830-27 and 6830-22) are characterized by a different iron oxidation degree (Table 4). In particular, in NS 6830-22 – which is cobalt blue – iron is more reduced. This could be ascribed to the deliberate addition of Co-bearing materials (for instance sulphide), which induced – as a secondary effect – the iron partial reduction.

Concerning BAS 46 and BAS 47 samples, it is interesting to note that both were deliberately decolorized, using antimony- and manganese-based decolorizers, respectively. However, the Mn-decolored glass (BAS 47) looks slightly greenish, while the Sb-decolored one (BAS 46) looks completely uncoloured. This suggests that Sb is more effective than Mn as oxidant. This conclusion is consistent with the results of the XANES analysis, which shows that iron in BAS46 is more oxidized than in BAS47 (Table 4).

The less oxidized samples belong to the primary natron glass series from the early Islamic tank furnace at Bet Eliezer (Israel), (in particular, samples BET EL3, 4 and 239) and to the series of glass coming from the Roman glass workshop excavated in Basinghall Street, London (specifically, samples BAS4, 56, 63 and 71). In these findings, iron is approximately equally distributed over the 2+ and 3+ oxidation states. The presence of partially reduced iron in sample BAS 71 is in contrast with its colour, which was supposed to be due to the oxidised species. It is interesting to note that the bluish glass BET EL 2 – showing a significant level of Fe³⁺ (68%) – has essentially the same elemental composition as the greenish/olive (BET EL 3) and the brown (BET EL 4) samples, which are, on the contrary, more reduced. This suggests that these last two glasses were produced in furnace regions with less access to air. Concerning the amber glass BET EL 239, it is the most reduced among the BET EL samples.

Finally, the XANES data on the chunk from Baniyas (Israel) indicate that iron is fully oxidized, as a result of the deliberate addition of a high amount of Mn dioxide. The purple color of this glass suggests the presence of Mn³⁺. However, other glasses (e.g. BAS 47, NS-6830-27) which have larger excesses of manganese over iron (Table 2) are not purple, suggesting that furnace atmosphere, as well as manganese content, may have influenced the oxidation state in this case.

Overall, these results suggest that primary natron glass was typically produced under moderately reducing conditions, where Fe³⁺ represents 50-70% of the total iron. More oxidised glasses appear to have been produced by adding an oxidising agent such as manganese or antimony oxide to the glass. The results from the workshop at Basinghall Street suggest that remelting and

blowing the primary glass into vessels had a relatively minor effect on its oxidation state. Further work on well-contextualised material is needed to clarify these issues.

1
2
3
4
5
6
7
8
9
10
11
12
13
14
15
16
17
18
19
20
21
22
23
24
25
26
27
28
29
30
31
32
33
34
35
36
37
38
39
40
41
42
43
44
45
46
47
48
49
50
51
52
53
54
55
56
57
58
59
60
61
62
63
64
65

ACKNOWLEDGEMENTS

The authors are grateful to BM08 GILDA beamline staff (ESRF, Grenoble) for the assistance during the XANES experiments.

Figure captions

Figure 1 – Picture of selected glass samples.

Figure 2 - Normalized Fe *K*-pre-edge spectra and the best fit model calculated for (a) the reference compounds and (b) the glass samples.

Figure 3 – Normalized Mn *K*-pre-edge spectra and the best fit model calculated for (a) the reference compounds and (b) the glass samples.

Figure 4 - Plot of $I(\text{Fe}^{3+})/[I(\text{Fe}^{2+}) + I(\text{Fe}^{3+})]$ vs. the pre-edge centroid positions, calculated by Fe *K*-edge XANES data.

-
- 1 [1] D. Dungworth, *The Historic Environment* 2, 21 (2011)
- 2 [2] M. Cotte, J. Susini, J. Dik, K. Janssens, *Accounts Chem. Res.* 43, 705 (2010)
- 3 [3] S. Quartieri S. (2011) *Synchrotron Radiation in Archaeological and Cultural Heritage Science.*
- 4 *XI School on Synchrotron Radiation: Fundamentals, Methods and Applications. Duino (Trieste -*
- 5 *Italy) 5 – 16 September 2011, <http://webusers.fis.uniroma3.it/sils/apertura.htm>.*
- 6 [4] R. Arletti, M.C. Dalconi, S. Quartieri, M. Triscari, G. Vezzalini, *Appl. Phys. A* 83, 239 (2006)
- 7 [5] R. Arletti R, G. Vezzalini, S. Quartieri, D. Ferrari, M. Merlini, M. Cotte, *Appl. Phys. A* 92, 127
- 8 (2008)
- 9 [6] R. Arletti, C. Giacobbe, S. Quartieri, G. Sabatino, G. Tigano, M. Triscari, G. Vezzalini,
- 10 *Archaeom.* 52, 99 (2010)
- 11 [7] R. Arletti, R., G. Vezzalini, S. Benati, L. Mazzeo Saracino, A. Gamberini, *Arch.* 52, 252
- 12 (2010)
- 13 [8] F. Farges, Y. Lefrere. S. Rossano, A. Berthereau, G. Calas, G.E. Brown, *J. Non-Cryst. Solids,*
- 14 344, 176 (2004)
- 15 [9] F. Farges, E. Chalmin, C. Vignaud, I. Pallot-Frossard, J. Susini, J. Bargar, G.E. Brown, M.
- 16 *Menu, Phys. Scripta* 115, 885 (2005)
- 17 [10] F. Farges, S. Djanarthany, S. de Wispelaere, M. Munoz, B. Magassouba, A. Haddi, M. Wilke,
- 18 C. Schmidt, M. Borchert, P. Trocellier, W. Crichton, A. Simionovici, P.E. Petit, M. Mezouar, M.P.
- 19 Etcheverry, I. Pallot-Frossard, J.R. Bargar, G.E. Brown, D. Grolimund, A. Scheidegger, *Phys.*
- 20 *Chem. Glasses,* 46, 350 (2005)
- 21 [11] L. Galois, G., Calas, M.A. Arrio, *Chem. Geol.,* 174, 307 (2001).
- 22 [12] G. Giuli, G. Pratesi, C. Cipriani, E. Paris, *Geochim. Cosmochim. Ac.* 66, 4347 (2002)
- 23 [13] G. Giuli, S.G. Eeckhout, E. Paris, C. Koeberl, G. Pratesi, *G. Meteorit. Planet. Sci.,* 40, 1575
- 24 (2005)
- 25 [14] G. Giuli, S.G. Eeckhout, C. Koeberl, G. Pratesi, E. Paris, *. Meteorit. Planet. Sci.* 43, 981 (2008)
- 26 [15] N. Métrich, J. Susini, E. Foy, F. Farges, D. Massare, L. Sylla, S. Lequien, M. Bonnin-Mosbah,
- 27 *Chem. Geol.* 231, 350 (2006)
- 28 [16] S. Quartieri, M. Triscari, G. Sabatino, F. Boscherini, A. Sani A. *Eur. J. Mineral.* 14, 749
- 29 (2002):
- 30 [17] S. Quartieri, M.P. Riccardi, B. Messiga, F. Boscherini, *J. Non-Cryst. Solids,* 351, 3013 (2005):
- 31 [18] S. Rossano, A. Ramos, J.-M. Delaye, S. Creux, A. Filipponi, C.H. Brouder, G. Calas, *Europhys.*
- 32 *Lett.* 49, 597 (2000)
- 33 [19] M. Wilke, G.M. Partzsch, R. Bernhardt, D. Lattard, *Chem. Geol.,* 213, 71 (2004)
- 34 [20] M. Wilke, G. Schmidt, F. Farges, V. Malavergne, L. Gautron, A. Simionovici, M. Hahn, P.E.
- 35 *Petit, Chem. Geol.,* 229, 144 (2006)
- 36 [21] M. Wilke, F. Farges, G.M. Partzsch, C. Schmidt, H. Beherens, H. Am. *Mineral.* 92, 44 (2007)
- 37 [22] A. Santagostino Barbone, E. Gliozzo, F. D'acapito, I. Turbanti Memmi, M. Turchiano,
- 38 *G. Volpe, Archaeom.* 50, 389 (2010)
- 39 [23] L. De Ferri, R. Arletti, G. Ponterini, S. Quartieri, *Eur. J. Mineral.* 23, 969 (2011)
- 40 [24] E. Chalmin, F. Farges, G.E. Brown, *Contrib. Mineral. Petrol.* 157, 111 (2009)
- 41 [25] O. Schalm, K. Proost, K. De Vis, S. Cagno, K. Janssens, F. Mees, P. Jacobs, J. Caen, *Arch.*
- 42 (2010) doi: 10.1111/j.1475-4754.2010.00534.x
- 43 [26] S. Cagno, G. Nuyts, S. Bugani, K. De Vis, O. Schalm, J. Caen, L. Helfen, M. Cotte, P.
- 44 *Reischig, K. Janssens, J. Anal. At. Spectrom.* 26, 2442 (2011)
- 45 [27] I.C. Freestone, Y. Gorin-Rosen Y., M.J. Hughes in *Ateliers primaires et secondaires de verriers*
- 46 *du second millinaire av. J.-C. au Moyen-Age, ed. By M.-D. Nenna (Travaux de la Maison de*
- 47 *l'Orient Méditerranéen 2000) p. 65*
- 48 [28] I.C. Freestone, S. Wolf, M. Thirlwall, *Annales du 16e Congres de l'Association Internationale*
- 49 *pour l'Histoire du Verre,* 153 (2005)
- 50
- 51
- 52
- 53
- 54
- 55
- 56
- 57
- 58
- 59
- 60
- 61
- 62
- 63
- 64
- 65

1 [29] I.C. Freestone, I.C. 1994, in Excavations at Carthage, Vol II, ed. By H. Hurs (Oxford Univ
2 Press for British Academy. 1994), p. 290.
3 [30] I.C. Freestone, R. Greenwood, Y. Gorin-Rosen in Hyalos - Vitrum - Glass. History
4 Technology and Conservation of glass and vitreous materials in the Hellenic World. 1st
5 International conference Rhodes – Greece, ed. By G. Kordas (2002) p. 167.
6 [31] S. Pascarelli, F. Boscherini, F. D’Acapito, J. Hardy, C. Meneghini, S. Mobilio, J. Synch. Rad.
7 3, 147 (1996)
8 [32] PeakFit4 – Systat Software.Inc, www.systat.com/products/PeakFit/
9 [33] A.J. Berry, H.St.C. O’Neill, K.D. Jayasuriya, S.J. Campbell, G.J. Foran, Am. Mineral., 88, 967
10 (2003)
11 [34] M. Wilke, F. Farges, P.E. Petit, G.E. Brown, F. Martin, Am. Mineral. 86, 714 (2001)
12 [35] G.A. Waychunas, M.J. Apter, G.E. Brown, Phys. Chem. Min. 10, 1 (1983)
13 [36] T.E. Westre, P. Kennepohl, J. de Witt, B. Hedman, K.O. Hodgson, E.I., Solomon, J. Am.
14 Chem. Soc. 119, 6297 (1997)
15
16
17
18
19
20
21
22
23
24
25
26
27
28
29
30
31
32
33
34
35
36
37
38
39
40
41
42
43
44
45
46
47
48
49
50
51
52
53
54
55
56
57
58
59
60
61
62
63
64
65

Table 1 - Selected information on provenance, color, typology and chemistry of the studied ancient glass samples.

Sample	Provenance	Color	Description
BET EL 6831-1	Bet Eliezier	Blue green	Chunk from tank furnace
BET EL 2	Bet Eliezier	Blue green	Chunk from tank furnace
BET EL 3	Bet Eliezier	Green	Chunk from tank furnace
BET EL 4	Bet Eliezier	Brown	Chunk from tank furnace
BET EL 239	Bet Eliezier	Amber	Chunk from tank furnace
BAS 4	London	Green-blue	Lump of raw glass
BAS 46	London	Colorless	Moil
BAS 47	London	Colorless	Moil
BAS 56	London	Green blue	Moil
BAS 63	London	Green blue	Moil
BAS 71	London	Yellow-green	Moil
Carthage	Carthage	Green-olive	Chunk
NS 6830-27	North Sinai	Green -olive	Chunk from tank furnace
NS 6830-22	North Sinai	Cobalt blue	Vessel
Banias	Banias	Purple	Chunk from tank furnace

Table 2

Table 2: Chemical data of the analysed samples. All the data are reported as wt % with the exclusion of Cu and Co (ppm)

Abbreviations: b.d.: below detection limit, n.a.: not analysed

Sample	SiO ₂	TiO ₂	Al ₂ O ₃	MgO	MnO	Fe ₂ O ₃	CaO	Na ₂ O	K ₂ O	Cl	SO ₃	P ₂ O ₅	Sb ₂ O ₃	Cu ppm	Co ppm
BET EL 6831-1	75.98	<0.10	3.29	0.57	0.02	0.49	5.96	12.14	0.40	0.70	0.15	<0.10	n.d.	9	1
BET EL 2	73.65	0.16	3.70	0.68	0.02	0.94	6.65	13.01	0.55	0.54	0.12	<0.10	<0.1	21	2
BET EL 3	74.95	0.13	3.36	0.58	0.02	0.58	7.27	11.36	0.46	0.68	0.14	<0.10	<0.1	25	1
BET EL 4	75.98	<0.10	3.06	0.61	0.01	0.39	7.63	11.27	0.43	0.69	0.18	<0.10	<0.1	9	2
BET EL 239	72.85	0.12	3.63	0.51	<0.10	0.64	7.98	13.04	0.47	0.79	<0.1	<0.10	<0.1	n.a.	n.a.
BAS 4	70.85	0.05	2.19	0.51	0.26	0.42	8.29	15.11	0.66	0.99	0.23	0.21	b.d.	3	3
BAS 46	68.96	0.03	1.66	0.40	0.01	0.42	6.37	19.06	0.38	1.36	0.40	0.04	0.79	13	2
BAS 47	70.29	0.02	2.15	0.56	1.34	0.31	7.90	15.57	0.54	1.11	0.19	0.10	b.d.	18	11
BAS 56	70.88	0.09	2.41	0.51	0.52	0.46	7.50	15.94	0.60	1.02	0.24	0.06	b.d.	37	10
BAS 63	70.49	0.10	2.31	0.41	0.54	0.31	7.96	16.25	0.44	1.21	0.30	-0.01	b.d.	3	6
BAS 71	70.37	0.14	2.41	0.54	0.51	0.48	7.50	15.13	0.57	1.04	0.18	0.05	0.62	28	11
Carthage 32832	64.23	0.71	3.28	1.21	1.6	3.65	5.00	18.39	0.46	1.03	0.14	<0.10	<0.1	65	14
NS 6830-27	66.08	0.36	2.49	1.14	2.63	1.33	5.56	17.58	0.47	0.96	0.35	<0.10	<0.1	65	11
NS 6830-22	65.69	0.39	2.67	1.14	0.42	2.42	5.98	17.95	0.49	0.97	0.44	<0.10	<0.1	~0.1	~0.1
Banias 62	71.70	0.19	0.87	2.71	0.95	0.36	7.61	12.76	1.84	0.88	0.27	0.27	b.d.	n.a.	4

Table 2 - Fe and Mn K-edge XANES feature positions of the reference compounds.

Sample	Fe oxidation state	Coordination	Component position (eV)	Area	Total Area	Centroid position (eV)	R ²																																																																																																																															
Almandine	2 ⁺	VIII	7112.30	0.0252	0.0332	7112.69	0.9976																																																																																																																															
			7113.92	0.0079				Olivine	2 ⁺	VI	7111.73	0.0192	0.0340	7112.25	0.9993	7112.50	0.0097	7113.77	0.0051	Hercynite	2 ⁺	IV	7112.25	0.1232	0.1752	7112.67	0.9990	7113.67	0.0520	ST1	33% 2 ⁺ 67% 3 ⁺		7112.47	0.0495	0.1404	7113.51	0.9992				7114.08	0.0909	Magnetite	2 ⁺	VI	7113.31	0.0339	0.1537	7114.06	0.9987	3 ⁺	IV-VI	7113.94	0.0877	Hematite	3 ⁺	VI	7113.45	0.0291	0.1106	7114.97	0.9997	7114.67	0.0427	7115.71	0.0191	7116.70	0.0110	7117.67	0.0086	Silicalite	3 ⁺	IV	7114.18	0.3036	0.3036	7114.18	0.9979	Sample	Mn oxidation state	Coordination	Component position (eV)	Area	Total Area	Centroid position (eV)	R ²	Rhodocrosite	2+	VI	6539.21	0.0206	0.0390	6539.60	0.9985	6540.05	0.0184	Tephroite	2+	VI	6538.83	0.0261	0.1434	6539.38	0.9989	6539.50	0.1174	MnO	2+	VI	6539.19	0.0226	0.0416	6539.55	0.9985	6539.99	0.0190	Mn ₂ O ₃	3+	VI	6539.55	0.0570	0.1107	6540.70	0.9990	6541.30	0.0305	6542.74	0.0232	MnO ₂	4+	VI	6540.30	0.0474	0.1668
Olivine	2 ⁺	VI	7111.73	0.0192	0.0340	7112.25	0.9993																																																																																																																															
			7112.50	0.0097																																																																																																																																		
			7113.77	0.0051																																																																																																																																		
Hercynite	2 ⁺	IV	7112.25	0.1232	0.1752	7112.67	0.9990																																																																																																																															
			7113.67	0.0520																																																																																																																																		
ST1	33% 2 ⁺ 67% 3 ⁺		7112.47	0.0495	0.1404	7113.51	0.9992																																																																																																																															
			7114.08	0.0909																																																																																																																																		
Magnetite	2 ⁺	VI	7113.31	0.0339	0.1537	7114.06	0.9987																																																																																																																															
	3 ⁺	IV-VI	7113.94	0.0877																																																																																																																																		
Hematite	3 ⁺	VI	7113.45	0.0291	0.1106	7114.97	0.9997																																																																																																																															
			7114.67	0.0427																																																																																																																																		
			7115.71	0.0191																																																																																																																																		
			7116.70	0.0110																																																																																																																																		
			7117.67	0.0086																																																																																																																																		
Silicalite	3 ⁺	IV	7114.18	0.3036	0.3036	7114.18	0.9979																																																																																																																															
Sample	Mn oxidation state	Coordination	Component position (eV)	Area	Total Area	Centroid position (eV)	R ²																																																																																																																															
Rhodocrosite	2+	VI	6539.21	0.0206	0.0390	6539.60	0.9985																																																																																																																															
			6540.05	0.0184																																																																																																																																		
Tephroite	2+	VI	6538.83	0.0261	0.1434	6539.38	0.9989																																																																																																																															
			6539.50	0.1174																																																																																																																																		
MnO	2+	VI	6539.19	0.0226	0.0416	6539.55	0.9985																																																																																																																															
			6539.99	0.0190																																																																																																																																		
Mn ₂ O ₃	3+	VI	6539.55	0.0570	0.1107	6540.70	0.9990																																																																																																																															
			6541.30	0.0305																																																																																																																																		
			6542.74	0.0232																																																																																																																																		
MnO ₂	4+	VI	6540.30	0.0474	0.1668	6541.95	0.9986																																																																																																																															
			6542.14	0.0895																																																																																																																																		
			6543.98	0.0300																																																																																																																																		

Table 3 - Fe and Mn K-edge XANES feature positions in the ancient glass samples.

Sample	Component position (eV)	Area%	Total Area	Centroid position (eV)	R ²	$\frac{I(\text{Fe}^{3+})}{I(\text{Fe}^{2+}) + I(\text{Fe}^{3+})}$	Fe ³⁺ %
Fe K-edge							
BET EL 6831-1	7112.39	28.462	0.1578	7113.60	0.9996	0.690	70
	7114.09	71.538					
BET EL 2	7111.85	11.525	0.1155	7113.65	0.9983	0.676	68
	7112.89	30.101					
	7114.39	58.373					
BET EL 3	7112.16	26.109	0.0886	7113.41	0.9986	0.582	56
	7113.13	31.843					
	7114.40	42.048					
BET EL 4	7111.93	24.664	0.08593	7113.23	0.9987	0.580	55
	7112.99	36.594					
	7114.29	38.742					
BET EL 239	7111.78	20.234	0.08210	7113.12	0.9995	0.510	46
	7112.82	42.417					
	7114.20	37.349					
BAS 4	7112.00	23.198	0.0991	7113.33	0.9995	0.580	55
	7112.99	32.567					
	7114.29	44.235					
BAS 46	7112.80	18.239	0.1212	7114.17	0.9994	0.879	96
	7114.08	45.514					
	7114.99	36.247					
BAS 47	7112.47	22.721	0.1437	7114.00	0.9992	0.749	78
	7114.19	55.787					
	7115.11	21.492					
BAS 56	7111.90	23.763	0.0774	7113.25	0.9990	0.566	54
	7113.04	34.702					
	7114.19	41.535					
BAS 63	7111.87	22.123	0.1110	7113.21	0.9991	0.545	51
	7112.79	33.698					
	7114.20	44.183					
BAS 71	7111.92	12.036	0.0708	7113.37	0.9991	0.586	56
	7112.77	38.291					
	7114.19	49.673					

Carthage	7112.53	7.3259	0.1797	7114.00	0.9993	0.883	96
	7114.12	92.674					
NS 6830-27	7112.68	8.7434	0.1861	7113.96	0.9987	0.878	96
	7114.05	84.180					
	7114.42	7.0762					
NS 6830-22	7112.61	31.905	0.1268	7113.78	0.9988	0.680	69
	7114.32	52.043					
	7114.40	16.052					
Banias	7112.99	11.861	0.1748	7114.06	0.9996	0.887	97
	7114.20	88.139					
Mn K-edge							
BAS 4	6538.84	27.809	0.0968	6539.50	0.9988		
	6539.75	72.191					
BAS 47	6538.96	28.703	0.0897	6539.68	0.9991		
	6539.98	71.297					
BAS 56	6538.84	24.787	0.0947	6539.57	0.9989		
	6539.81	75.213					
BAS 63	6538.95	38.203	0.0902	6539.52	0.9985		
	6539.88	61.796					
BAS 71	6538.90	27.291	0.0954	6539.29	0.9994		
	6539.87	72.709					
Carthage	6539.60	100	0.1127	6539.60	0.9990		
NS 6830-27	6539.64	100	0.1182	6539.64	0.9987		
NS 6830-22	6538.86	25.662	0.0904	6539.58	0.9990		
	6539.82	74.337					
Banias	6539.64	100	0.1179	6539.64	0.9992		

Figure

[Click here to download high resolution image](#)



BET EL 2



BET EL 3



BET EL 4



BET EL 239



BAS 47



BAS 56



BAS 63



BAS 71

Figure 2a

[Click here to download high resolution image](#)

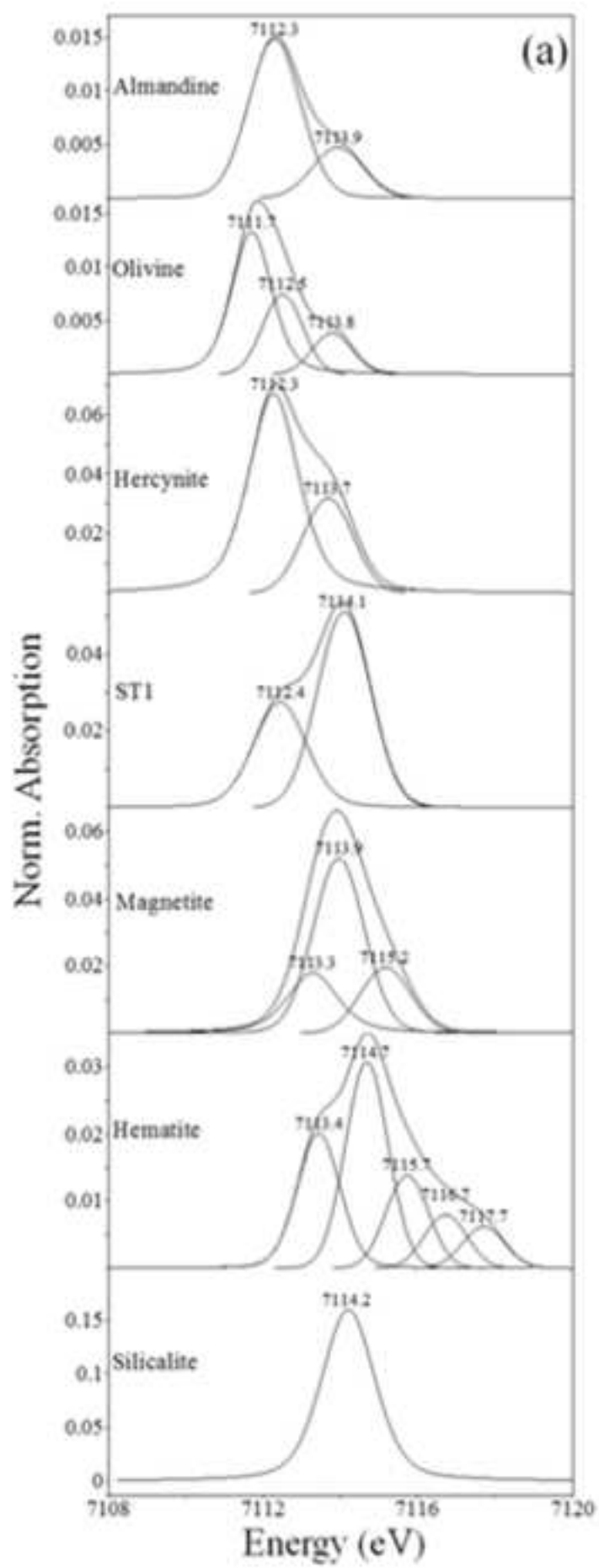


Figure 2b
[Click here to download high resolution image](#)

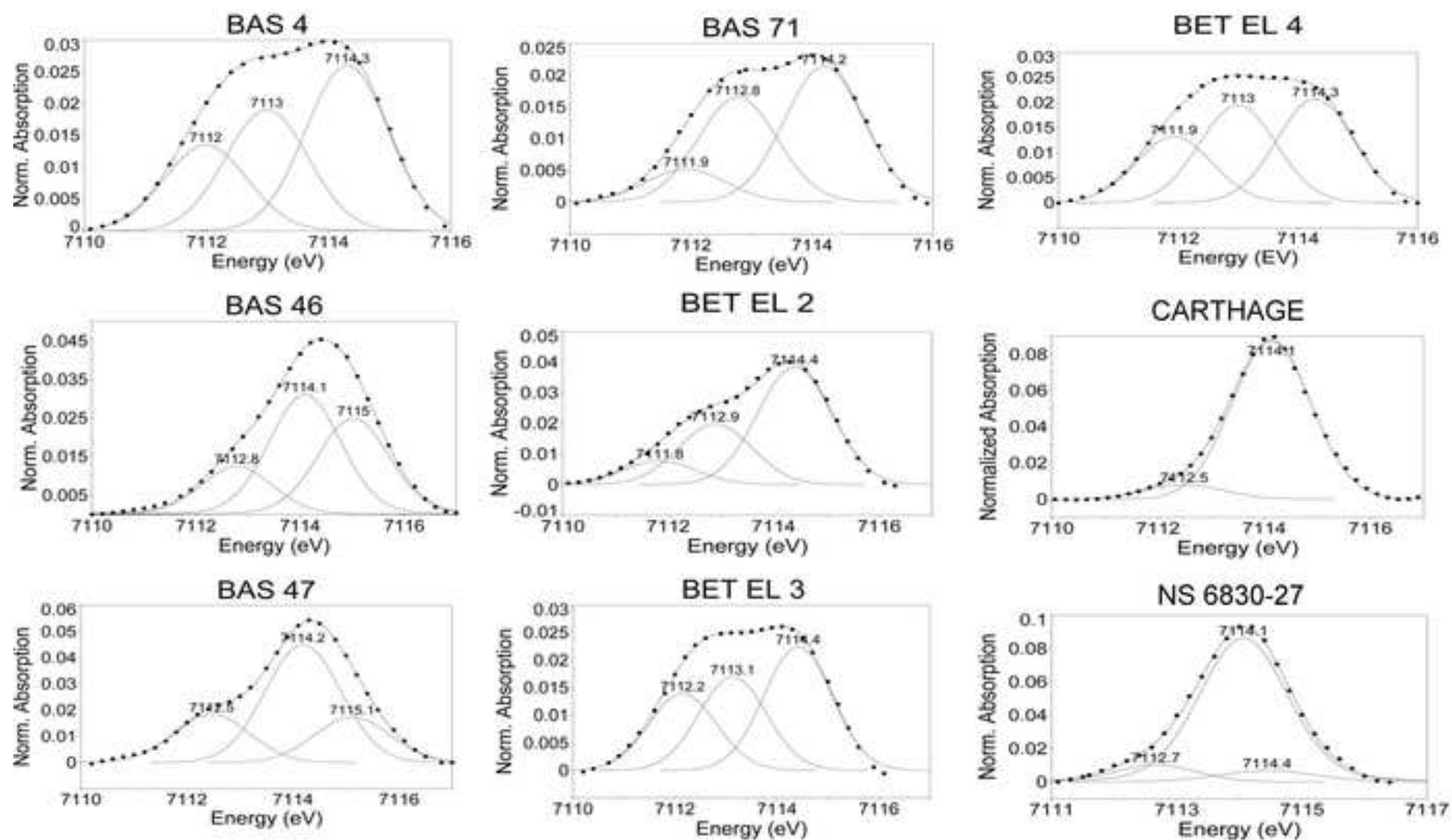


Figure 3a

[Click here to download high resolution image](#)

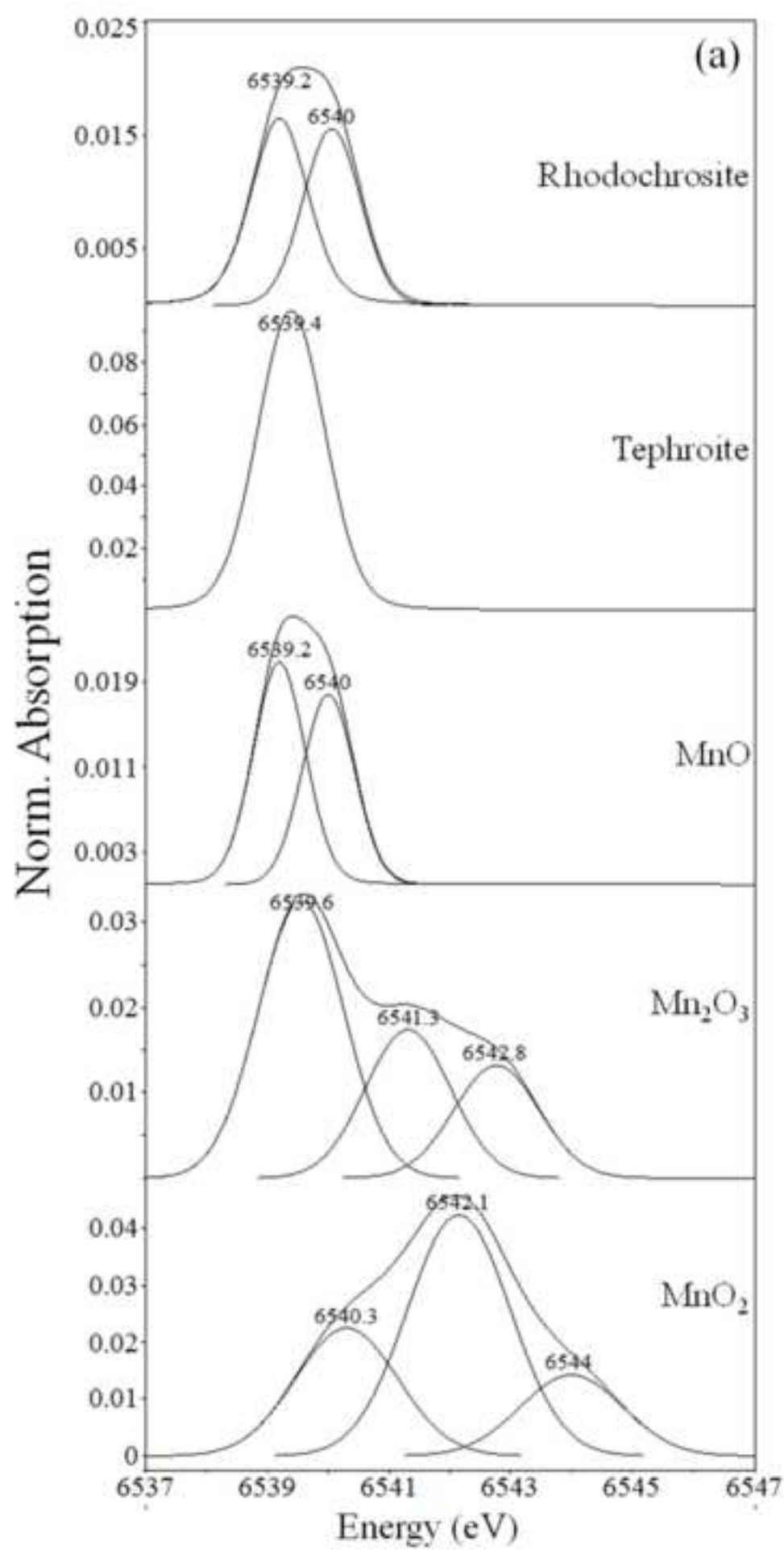


Figure 3b
[Click here to download high resolution image](#)

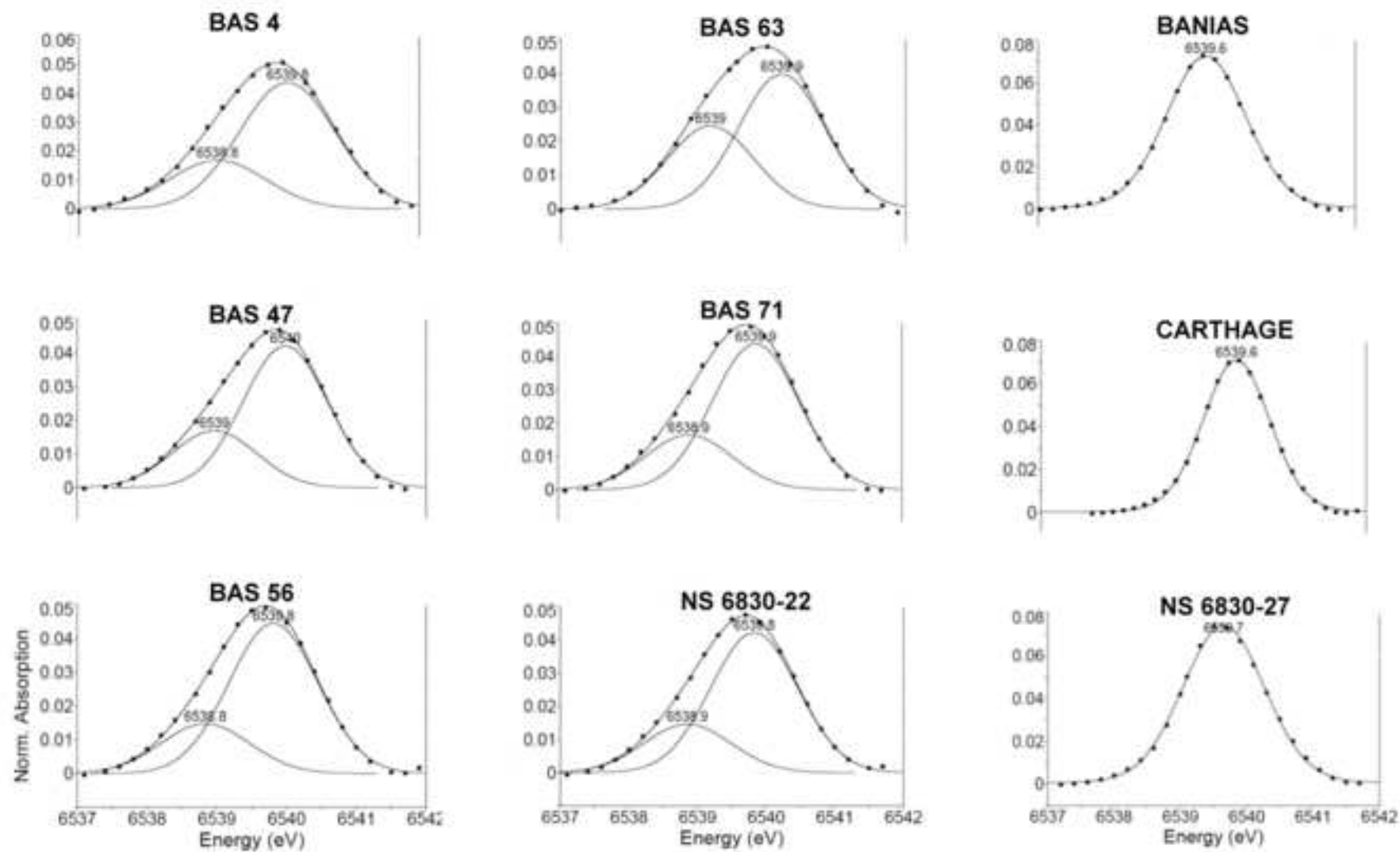


Figure 4rev
[Click here to download high resolution image](#)

